GPS Solut (2011) 15:415–425
DOI 10.1007/s10291-010-0200-x

ORIGINAL ARTICLE

# Assessment of ZTD derived from ECMWF/NCEP data with GPS ZTD over China

**Qinming Chen · Shuli Song · Stefan Heise · Yuei-An Liou · Wenyao Zhu · Jingyang Zhao**

Received: 27 March 2010 / Accepted: 2 December 2010 / Published online: 5 January 2011


**Abstract** The accuracy and feasibility of computing the zenith tropospheric delays (ZTDs) from data of the European Center for Medium-Range Weather Forecasts (ECMWF) and the United States National Centers for Environmental Prediction (NCEP) are studied. The ZTDs are calculated from ECMWF/NCEP pressure-level data by integration and from the surface data with the Saastamoinen model method and then compared with the solutions measured from 28 global positioning system (GPS) stations of the Crustal Movement Observation Network of China (CMONOC) for 1 year. The results are as follows: (1) the error of the integration method is 1–3 cm less than that of the Saastamoinen model method. The agreement between the ECMWF ZTD and GPS ZTD is better than that between NCEP ZTD and GPS ZTD; (2) the bias and root mean square difference (RMSD), especially the latter, have a seasonal variation, and the RMSD decreases with increasing altitude while the variation with latitude is not obvious; and (3) when using the full horizontal resolution of 0.5° × 0.5° of the ECMWF meteorological data in place of a reduced 2.5° × 2.5° grid, the mean RMSD between GPS and ECMWF ZTD decreases by 4.5 mm. These results illuminated the accuracy and feasibility of computing the tropospheric delays and establishing the ZTD prediction model over China for navigation and positioning with ECMWF and NCEP data.

**Keywords** GPS · Zenith tropospheric delay (ZTD) · CMONOC · ECMWF · NCEP

**Abbreviations**

| | |
|---|---|
| CMONOC | The crustal movement observation network of China |
| CDAS | Climate data assimilation system |
| ECMWF | The European center for medium-range weather forecasts |
| ECMWF ZTD | The zenith tropospheric delay derived from ECMWF data |
| GPS | Global positioning system |
| GPS ZTD | GPS observed zenith tropospheric delay |
| GDAS | Global data assimilation system |
| HIRLAM | The high-resolution limited area model |
| IFS | Integrated forecast system |
| int | The integral method |

Q. Chen · S. Song (✉) · W. Zhu · J. Zhao
Shanghai Astronomical Observatory,
Chinese Academy of Sciences, Shanghai, China
e-mail: slsong@shao.ac.cn

W. Zhu
e-mail: zhuw@shao.ac.cn

J. Zhao
e-mail: zhaojingyang@shao.ac.cn

Q. Chen · J. Zhao
Graduate School of the Chinese Academy of Sciences,
Beijing, China
e-mail: qmchen@shao.ac.cn

Q. Chen
Southwest University of Science and Technology,
Mianyang, Sichuan Province, China

S. Heise
Helmholtz Centre Potsdam, GFZ German Research
Centre for Geosciences, Potsdam, Germany
e-mail: stefan.heise@gfz-potsdam.de

Y.-A. Liou (✉)
Center for Space and Remote Sensing Research,
National Central University, Jhongli, Taiwan
e-mail: yueian@csrsr.ncu.edu.tw

| | |
|---|---|
| IGS | International GNSS Service |
| NCEP | The United States National Centers for environmental prediction |
| NCEP ZTD | The zenith tropospheric delay derived from NCEP data |
| NWM | Numerical weather model |
| NWP | Numerical weather prediction |
| RMSD | Root mean square difference |
| saas | The Saastamoinen method |
| ZTD | The zenith tropospheric delay |

## Introduction

The ionosphere and the neutral atmosphere have a large impact on global positioning system (GPS) observations. The impact of the ionosphere can reach 10 m in the zenith direction and may be more than 50 m at 5° elevation. Dual-frequency observations can be combined to eliminate the ionospheric effect. As to the neutral atmospheric delay, the term "tropospheric delay" comprises the troposphere and the stratosphere delay because the troposphere contains most of the mass of the neutral atmosphere and practically all of the water vapors. The tropospheric delay of GPS signals from the zenith to the horizon is about 2–20 m and cannot be corrected by dual-frequency observations. Thus, the effect of neutral atmosphere must be considered carefully for navigation and positioning.

Many researchers have used the zenith tropospheric delay (ZTD) derived from meteorological data to validate ZTD measured by GPS and concluded that they basically agreed with each other (Liou et al. 2000, 2001; Liou and Huang 2000; Shuli et al. 2004, 2005; Vedel et al. 2001; Haase et al. 2001; Walpersdorf et al. 2007). This supports the feasibility and reliability of the GPS ZTD. Conversely, researchers are beginning to use the high-precision GPS ZTD to validate ZTDs derived from the meteorological data acquired by a number of meteorological observation systems (Andrei and Chen 2008; Guerova et al. 2003).

Vedel et al. (2001) compared the ZTDs derived from radiosonde and numerical weather prediction (NWP) model HIRLAM (high-resolution limited area model) with those determined by 150 IGS GPS stations. They found that the GPS ZTD was highly correlative with those derived from the meteorological data, especially with those measured by the radiosondes. Apparently, GPS ZTD is considered as a new data source for validating NWP models. In order to assess the applicability of the numerical weather model (NWM) of the global data assimilation system (GDAS) on real-time navigation, Andrei and Chen (2008) evaluated the ZTD calculated from NWM extracted meteorological parameters through comparison with those derived from the 18 International GNSS Service (IGS) GPS stations. They found that the root mean square difference (RMSD) is about 3 cm, with a largest RMSD of 5.5 cm and largest deviation of 4.5 cm, implying that the accuracy of the NWM ZTD of the GDAS system meets the needs of GPS navigation.

The analysis or reanalysis data from the European Center for Medium-Range Weather Forecasts (ECMWF) or the United States National Centers for Environmental Prediction (NCEP) are of high quality over the regions with sufficient dense data, but the accuracy is uncertain over areas with sparse observations (Bromwich and Wang 2005). Some studies have been done using ECMWF and NCEP data to correct tropospheric delay for satellite navigation and positioning, and some improved tropospheric delay correction models were established for North America (Pany et al. 2001; Ghoddousi-Fard et al. 2009; Ibrahim and El-Rabbany 2008). With the development of navigation and positioning in China, it is necessary to check the feasibility of ECMWF/NCEP data for tropospheric delay correction over China. We used ZTDs measured by 28 GPS stations of the Crustal Movement Observation Network of China (CMONOC) in 2004 to validate those derived from the ECMWF analysis, NCEP reanalysis, and forecast meteorological data. The feasibility and accuracy of the ECMWF/NCEP data are assessed for tropospheric delay correction, which is used to establish the ZTD correction model in China for navigation and positioning users with high accuracy requirements.

## The data

We mainly use the meteorological data from the ECMWF and the NCEP. The main objects of the ECMWF are the development of numerical methods for medium-range weather forecasting. The pressure-level and surface meteorological data of ECMWF from the IFS (Integrated Forecast System) are used. The time resolution of the data is 6 h, namely at 0, 6, 12, 18 UTC (Pernigotti et al. 2007). The data used in this study has a horizontal resolution of $0.5° \times 0.5°$ and a vertical resolution of 60 pressure levels reaching 0.1 mbar at the top level. The pressure-level meteorological data are altitude, air temperature, specific humidity, and pressure. The surface meteorological data include surface pressure, dewpoint temperature at 2 m, and temperature at 2 m. The latitude range of the data is from 15°N to 54.5°N and longitude range is from 70°E to 139.5°E.

The NCEP/NCAR Reanalysis Project began in 1991 as an outgrowth of the NCEP Climate Data Assimilation System (CDAS) project. The motivation for the CDAS

project was the "climate changes" which resulted from many changes introduced in the NCEP operational GDAS over the last decades in order to improve the forecasts. The NCEP/NCAR Reanalysis Project is using a state-of-the-art analysis/forecast system to perform data assimilation using past data from 1948 to the present (Kalnay et al. 1996). The reanalysis data have a horizontal resolution of 2.5° × 2.5° with a vertical resolution of 17 pressure levels reaching 10 mbar at the top level. The temporal resolution, the latitude, and longitude range of the data are similar for the ECMWF data. The pressure-level data used in the study include atmospheric pressure, temperature, geopotential height, and specific humidity. The surface data include surface geopotential height, and 2-m dewpoint temperature, and pressure. The NCEP forecast data contain mainly surface meteorological data such as pressure, temperature, and relative humidity. The latitude and longitude range and horizontal resolutions are similar to the NCEP reanalysis data. The temporal resolution of the NCEP forecast data is 12 h, which means the meteorological data are generated at 12 and 24 UTC.

The ECMWF/NCEP ZTDs are compared to GPS ZTDs from CMONOC stations. CMONOC is a national scientific infrastructure aiming to monitor the current intraplate deformation in China, using primarily the space geodetic techniques such as Very Long Baseline Interferometry (VLBI), Satellite Laser Ranging (SLR), and GPS (Wang and Zhang 2001). Currently, CMONOC consists of 30 GPS stations as shown in Fig. 1. Twenty-eight GPS stations were used in this research except CHAN and HRBN.

The CMONOC GPS ZTD time series are retrieved by the software GAMIT/GLOBK, developed by Massachusetts Institute of Technology (MIT) and the Scripps Institute of Oceanography (SIO) (Herring et al. 2006). The Piecewise Linear model is used to describe the ZTD and horizontal gradient. The ZTD is estimated every 2 h. Figure 1 shows the yearly mean ZTD of each GPS station in 2004.

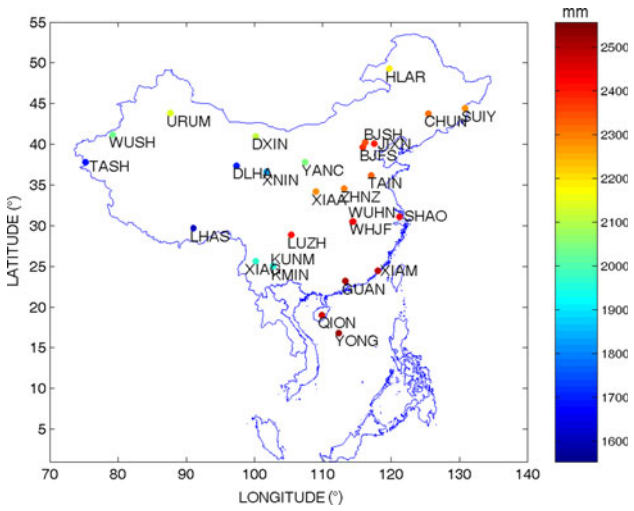


**Fig. 1** Distribution and mean ZTD in 2004 for CMONOC GPS stations. The surface color of the circle represents the mean ZTD for each station

## Deriving ZTD from ECMWF/NCEP meteorological data at GPS stations

Calculating the ZTD from ECMWF/NCEP meteorological data at a GPS station includes two steps—deriving the ZTD for each grid point from ECMWF/NCEP meteorological data and then calculating the ZTD at the GPS stations from the ZTD of the grid points.

## ZTD from ECMWF/NCEP meteorological data

Two methods are used to calculate the ZTD from ECMWF/NCEP meteorological data: the integration method and the Saastamoinen model method.

The integration method is mainly used for the pressure-level data and based on the formula,

$$N = k_1(P - e)/T + k_2 \times e/T + k_3 \times e/T^2 \quad (1)$$

$$e = h \times P/0.622 \quad (2)$$

where $k_1 = 77.604$ K/Pa, $k_2 = 64.79$ K/Pa, and $k_3 = 377600.0$ K$^2$/Pa, $N$ is the total refraction, $P$ is the atmospheric pressure, $e$ is the vapor pressure, and $h$ is the specific humidity. After calculating the total refraction, the ZTD is derived by using the formula:

$$\mathrm{ZTD} = 10^{-6}\int_S Nds = 10^{-6}\sum_i N_i\Delta s_i \quad (3)$$

The Saastamoinen model method is mainly used for the surface meteorological data (Saastamioinen 1972),

$$\mathrm{ZTD} = 0.002277 \times \frac{\left[P_0 + (0.05 + \frac{1255}{T_0+273.15})e\right]}{f(\varphi, \mathrm{H})} \quad (4)$$

$$e = rh \times 6.11 \times 10^{\frac{7.5T_0}{T_0+273.15}} \quad (5)$$

$$f(\varphi, H) = 1 - 0.00266\cos 2\varphi - 0.00028H \quad (6)$$

where $P_0$ is the surface pressure, $T_0$ is the surface temperature, $e$ is the vapor pressure, $rh$ is the relative humidity, $\varphi$ is the latitude, and $H$ is the altitude above ellipsoid surface.

While the NCEP pressure-level meteorological data are distributed by 17 pressure levels with the top altitude at about 34 km, the ECMWF data are distributed by 60 pressure levels with the top altitude at about 60 km. After deriving the ZTD by integration method from the pressure-level meteorological data, the zenith delay above the top

level needs to be added especially for the NCEP data to make it comparable with GPS ZTD, which is the total integration along the signal path. Because there is no meteorological data above the top level, the Saastamoinen model is used to calculate the zenith delay above the top level, and the meteorological data of the top level is used as input values of the model.

## ZTD at the GPS station from the ZTD of grid points

The resolution of the original ECMWF data is 0.5° × 0.5°. We chose a horizontal resolution of 2.5° × 2.5° for ECMWF and NCEP to make them comparable. Since the GPS stations and the ECMWF/NCEP grid points are usually not collocated and have different altitudes, two methods are used to calculate the ZTD at GPS stations from the ECMWF/NCEP ZTD of the grid points. One is to select the ZTD of the grid point nearest to the GPS station, then add the altitude difference correction. The other is to choose ZTDs of four grid points near the GPS station, add the altitude difference corrections, and then interpolate the ZTD to the GPS station by a distance-weighted algorithm (Chao 1997). Comparing the results of the two methods, it is found that they are similar. Hence, the first method of nearest grid point is chosen.

The area of China is comprised of complex terrain with great undulations. The altitude difference between a GPS station and the nearest grid point is as much as 1–2 km, resulting in more than 30 cm ZTD variation. Therefore, it is necessary to add the altitude difference correction to the grid point ZTD when compared with GPS ZTD. The characteristics of ZTD variation at the vertical direction over China are studied. This was done by calculating the zenith delay of each level from ECMWF pressure-level data and then studying the ZTD variation with the altitude.

Figure 2 shows the ZTD variation with altitude at the nearest grid points of HLAR, SUIY, QION, and TASH stations. It is clear that the ZTD decreases while the altitude increases. The decreasing rate and acceleration at each grid point are deduced by second-order polynomial fit, and then the series are used in the altitude difference correction.

Figure 3 shows the comparison of GPS ZTD (at TASH station as an example) and the ECMWF ZTD with and without altitude difference correction. The results, again, show that it is important to apply the altitude difference correction for the ECMWF/NCEP ZTD when making the comparison with the GPS ZTD.

## Comparison of GPS ZTD and ECMWF/NCEP ZTD

After the data were processed by the methods discussed above, the biases and RMSDs are computed between GPS ZTDs and ECMWF/NCEP ZTDs. Table 1 shows the yearly bias and RMSD at GPS stations for the year 2004.

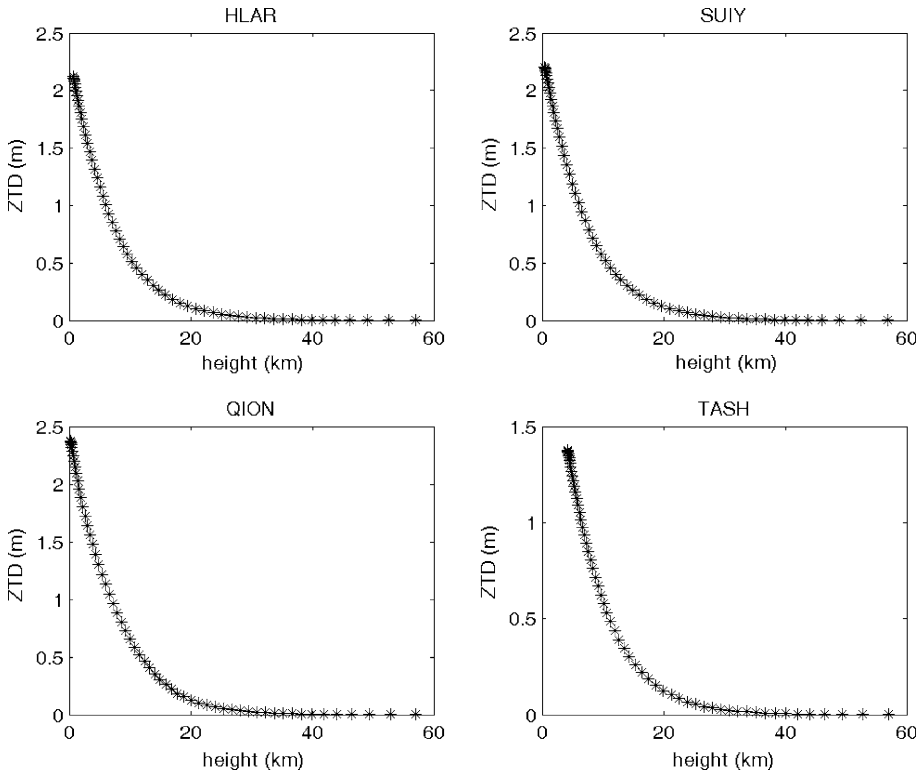


**Fig. 2** ZTD variation at the nearest grid points of the GPS stations (HLAR, SUIY, QION, and TASH) with altitude at 6:00 UTC, January 1, 2004

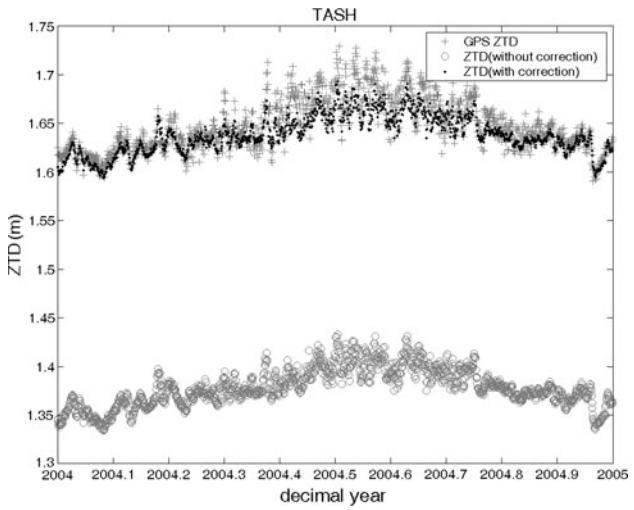


**Fig. 3** Comparison of GPS ZTD at station TASH with the ECMWF ZTD with and without altitude difference correction. The temporal resolution of the ZTD time series is 6 h

By comparing GPS ZTD and ECMWF ZTD, we see from Tables 1 and 2 that the bias and the RMSD of the ZTD as calculated by the integration method are

$$\mathrm{ZTD_{GPS}} - \mathrm{ZTD_{ECMWF(int)}} = -10.5 \pm 24.3 \text{ mm}.$$

The minimum bias is 0.6 mm (negative) at SUIY and the maximum is 28.6 mm (negative) at WUHN (Table 1). The corresponding minimum and maximum values of the RMSD are 10.8 and 35.4 mm, respectively (Table 2). The bias and RMSD of the ZTD calculated from ECMWF analysis data by the Saastamoinen model method are

$$\mathrm{ZTD_{GPS}} - \mathrm{ZTD_{ECMWF(saas)}} = 0.1 \pm 35.6 \text{ mm}.$$

The minimum value of the bias is 0.1 mm while the maximum is 34 mm (Table 1), and the minimum value of the RMSD is 14.2 mm while the maximum is 59.2 mm (Table 2).

By comparing GPS ZTD and NCEP ZTD, the bias and RMSD of ZTD calculated from NCEP reanalysis data by the integration method are

$$\mathrm{ZTD_{GPS}} - \mathrm{ZTD_{NCEP(int)}} = -8.5 \pm 33.0 \text{ mm}$$

The minimum value of the bias is 1.6 mm, the maximum 50.9 mm (negative) according to Table 1; the minimum value of RMSD is 16.8 mm, the maximum 53.6 mm (Table 2). The bias and RMSD of ZTD calculated from NCEP reanalysis data by the Saastamoinen model method are

$$\mathrm{ZTD_{GPS}} - \mathrm{ZTD_{NCEP(saas)}} = 22.1 \pm 51.1 \text{ mm}$$

The minimum value of the bias is 2.4 mm (negative), the maximum 86.1 mm (Table 1); the minimum value of RMSD is 24.9 mm, the maximum 99.9 mm (Table 2).

Comparing GPS ZTD and ZTD as calculated from NCEP forecast meteorological data gives

$$\mathrm{ZTD_{GPS}} - \mathrm{ZTD_{NCEP_{forecast(saas)}}} = 25.9 \pm 67.0 \text{ mm}.$$

The minimum value of the bias is 3.2 mm (negative), the maximum 111.9 mm. The minimum value of RMSD is 24.7 mm, the maximum 126.6 mm (Table 2).

Figures 4 and 5 show the yearly bias and the RMSD statistics by station. Tables 1 and 2 and these figures show that the agreement between the GPS ZTDs and the ECMWF ZTDs is better than that between GPS ZTDs and NCEP ZTDs. The accuracy of the integration method is better than that of the Saastamoinen method. The bias and RMSD of the ECMWF ZTD data calculated by the integration method are less than 4 cm. Even though the absolute value of the mean bias for the former (10.5 mm) is larger than the latter (0.1 mm), the residual variation range of the former is generally less than the latter. For example, as Table 1 and Fig. 6 show, the absolute bias of station WHJF by the integral method is 25.3 mm, which is larger than that of the Saastamoinen method (0.1 mm). However, the RMSD (32.7 mm) is less than that of the latter (54.2 mm), and the residual variation range is also less than that of the latter. Furthermore, the bias and RMSD between GPS ZTD and the ZTD derived from NCEP surface forecast meteorological data over China are less than 10 cm, except for station LUZH. The LUZH station is located in the Sichuan Basin, where the complexity of the surrounding terrain, weather changes, and the sparse NCEP data may result in larger bias and RMSD.

The temporal distributions of the bias and RMSD between GPS ZTD and ECMWF/NCEP ZTD are demonstrated in Figs. 7 and 8, which show the seasonal variations in terms of monthly statistics for bias and RMSD of GPS stations. These figures clearly show that the bias and RMSD, especially the RMSD, of the summer months are generally larger than those of the winter months. These characteristics are correlative to the complex and variable summer weather in China. The variability scales with the total water vapor amount, although different derivation schemes, such as GPS, Microwave Radiometer, and Radiosonde, are adopted, as demonstrated in Liou et al. (2001).

Our study of the spatial distribution is mainly focused on the variation characteristics of bias and RMSD with latitude and altitude. Figures 4 and 5 show the yearly bias and RMSD of 28 GPS stations with the latitude sorted by ascending order. From the charts, the connection between the precision and the latitude is not obvious.

In order to analyze the variation of the bias and RMSD with the station altitude, the altitude range was organized into six categories, namely 0–100 m, 100–500 m, 500–1,000 m, 1,000–2,000 m, 2,000–3,000 m, and above

**Table 1** Yearly bias and RMSD at GPS stations

| Station name | dis (km) | alt dif (m) | | GPS-ECMWF bias (mm) | | GPS-NCEP bias (mm) | | | GPS-ECMWF RMSD (mm) | | GPS-NCEP RMSD (mm) | | |
|---|---|---|---|---|---|---|---|---|---|---|---|---|---|
| | | GPS-ECMWF | GPS-NCEP | int | saas | int | saas | saas (fore) | int | saas | int | saas | saas (fore) |
| YONG | 28 | −26 | 28 | 2.7 | −2.5 | −3.7 | 53.9 | 31.7 | 19.6 | 46.6 | 29.6 | 76.0 | 57.2 |
| QION | 40 | 137 | 190 | −18.1 | 3.2 | −22.5 | 41.5 | 22.0 | 31.7 | 49.2 | 36.6 | 66.2 | 57.3 |
| GUAN | 91 | −105 | −246 | −7.4 | 21.6 | 12.0 | 66.8 | 72.3 | 23.1 | 54.5 | 30.3 | 85.6 | 96.2 |
| XIAM | 64 | −510 | −234 | 11.5 | 34.0 | 6.1 | 53.1 | 76.4 | 26.9 | 59.2 | 28.4 | 77.3 | 96.7 |
| KMIN | 29 | −54 | −28 | −9.3 | −6.4 | 9.6 | 9.0 | 40.7 | 14.7 | 32.0 | 22.7 | 36.4 | 61.9 |
| KUNM | 29 | −54 | −28 | −22.0 | −17.3 | −2.5 | −2.4 | 21.7 | 24.6 | 34.3 | 20.3 | 33.0 | 54.5 |
| XIAG | 38 | 32 | −50 | −23.7 | −18.5 | 1.6 | 3.5 | 28.6 | 27.5 | 35.7 | 24.1 | 37.0 | 57.1 |
| LUZH | 73 | −149 | −319 | −14.6 | 21.6 | 25.0 | 86.1 | 111.9 | 28.5 | 55.1 | 36.2 | 99.9 | 126.6 |
| LHAS | 108 | −1,684 | −1,618 | 7.0 | 1.1 | 6.9 | 7.2 | 31.7 | 22.7 | 20.0 | 24.0 | 25.4 | 46.4 |
| WHJF | 57 | −64 | 11 | −25.3 | 0.1 | −33.3 | 27.0 | 33.4 | 32.7 | 54.2 | 41.3 | 62.2 | 74.8 |
| WUHN | 68 | −110 | −35 | −28.6 | −5.5 | −34.5 | 22.4 | 31.7 | 35.4 | 52.8 | 42.1 | 57.6 | 73.8 |
| SHAO | 131 | −160 | −224 | −16.9 | 4.0 | −14.5 | 21.0 | 39.3 | 35.2 | 52.5 | 34.8 | 60.0 | 72.2 |
| XIAA | 107 | −184 | −498 | −11.6 | 7.3 | 19.5 | 53.0 | 53.3 | 23.8 | 39.3 | 29.6 | 67.7 | 88.9 |
| ZHNZ | 64 | −13 | −122 | −24.3 | −11.8 | −22.0 | 16.7 | 22.1 | 30.3 | 43.3 | 30.5 | 49.0 | 69.6 |
| TAIN | 86 | 148 | 269 | −18.6 | −13.6 | −33.8 | 10.0 | −6.4 | 32.9 | 41.6 | 44.4 | 43.5 | 61.4 |
| XNIN | 89 | −496 | −131 | −7.8 | −6.5 | −11.0 | 5.3 | 14.5 | 16.4 | 20.9 | 19.3 | 24.9 | 43.3 |
| DLHA | 13 | −754 | −1,056 | 2.1 | 3.2 | −50.9 | −41.0 | −31.6 | 10.8 | 14.2 | 52.8 | 45.7 | 42.9 |
| TASH | 27 | −1,407 | −1,032 | 9.0 | 3.5 | −31.8 | −30.3 | −5.6 | 15.3 | 14.2 | 35.2 | 34.5 | 24.7 |
| YANC | 20 | −256 | −97 | −20.8 | −16.9 | −23.9 | 8.3 | −11.8 | 23.7 | 30.8 | 29.0 | 32.7 | 63.6 |
| BJFS | 81 | −996 | −866 | 5.2 | 5.5 | 43.5 | 67.6 | 65.6 | 25.1 | 35.7 | 50.9 | 80.2 | 87.0 |
| JIXN | 6 | −189 | −427 | −7.2 | 0.2 | 17.3 | 47.8 | 34.9 | 15.4 | 31.2 | 28.2 | 63.7 | 68.1 |
| BJSH | 105 | −928 | −798 | 2.5 | 2.8 | 37.7 | 61.6 | 60.4 | 21.7 | 32.3 | 45.0 | 73.4 | 82.3 |
| DXIN | 73 | −341 | −1,074 | −17.0 | −1.6 | −3.5 | 13.2 | −3.2 | 21.9 | 19.2 | 16.8 | 27.9 | 55.9 |
| WUSH | 110 | 298 | 241 | −27.1 | −8.8 | −48.4 | −15.0 | −46.3 | 35.3 | 27.0 | 53.6 | 30.9 | 89.2 |
| CHUN | 100 | 69 | 140 | 2.5 | 12.8 | −19.4 | 11.2 | 12.2 | 22.3 | 32.3 | 29.2 | 36.1 | 52.1 |
| URUM | 93 | 326 | −59 | −26.2 | −12.0 | −46.0 | −12.9 | −12.6 | 32.2 | 26.2 | 49.8 | 34.3 | 73.8 |
| SUIY | 85 | −117 | −97 | −0.6 | 4.9 | −3.2 | 21.5 | 29.0 | 16.8 | 26.1 | 19.2 | 37.1 | 51.3 |
| HLAR | 65 | −110 | −248 | −9.1 | −0.4 | −13.0 | 13.9 | 10.5 | 14.7 | 17.6 | 19.6 | 31.5 | 46.8 |

The values were computed from the differences between the GPS ZTD and the ZTD derived from ECMWF/NCEP data with altitude difference correction at the nearest grid point. "dis" means the horizontal distance between the GPS station and the nearest grid point. "alt dif" refers altitude difference between the GPS station and the nearest grid point, "int" represents the integration method, "saas" is the abbreviation for Saastamoinen model method, and "fore" refers the forecast data

**Table 2** Yearly bias and RMSD statistics at GPS stations

| | GPS-ECMWF bias (mm) | | GPS-ECMWF RMSD (mm) | | GPS-NCEP bias (mm) | | | GPS-NCEP RMSD (mm) | | |
|---|---|---|---|---|---|---|---|---|---|---|
| | int | saas | int | saas | int | saas | saas (forecast) | int | saas | saas (forecast) |
| Mean | −10.5 | 0.1 | 24.3 | 35.6 | −8.5 | 22.1 | 25.9 | 33.0 | 51.1 | 67.0 |
| Minimum | −0.6 | 0.1 | 10.8 | 14.2 | 1.6 | −2.4 | −3.2 | 16.8 | 24.9 | 24.7 |
| Maximum | −28.6 | 34.0 | 35.4 | 59.2 | −50.9 | 86.1 | 111.9 | 53.6 | 99.9 | 126.6 |

The minimum and maximum values are given for the absolute values of the bias and the RMSD

3,000 m. The yearly bias and RMSD were calculated for each category. The variation of bias with the altitude of the station is shown in Fig. 9. The variation of bias with the altitude difference of GPS—grid point is shown in Fig. 10. The variation of RMSD with the station altitude is given in Fig. 11.

Figure 9 shows that the correlation between the bias and station altitude is not obvious. Moreover, the correlation

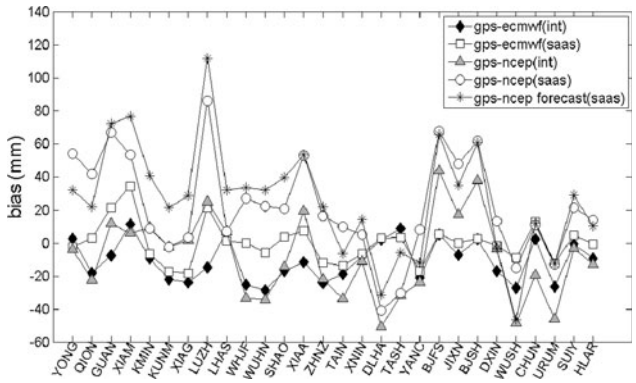


**Fig. 4** Comparison of yearly biases for 2004 between GPS ZTD and ECMWF/NCEP ZTD with integration method (int) and Saastamoinen method (saas) at GPS stations sorted in ascending latitude

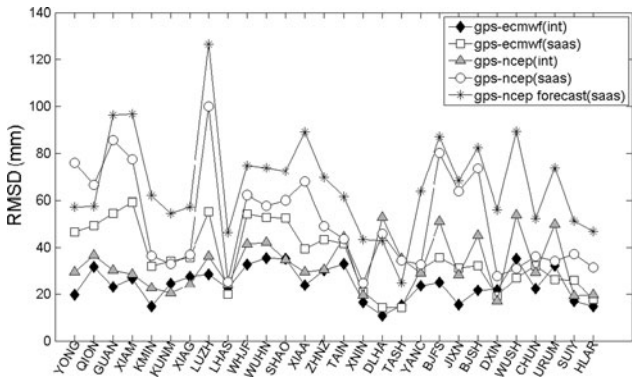


**Fig. 5** Comparison of yearly RMSD for 2004 between GPS ZTD and ECMWF/NCEP ZTD with integration method (int) and Saastamoinen method (saas) at GPS stations sorted in ascending latitude

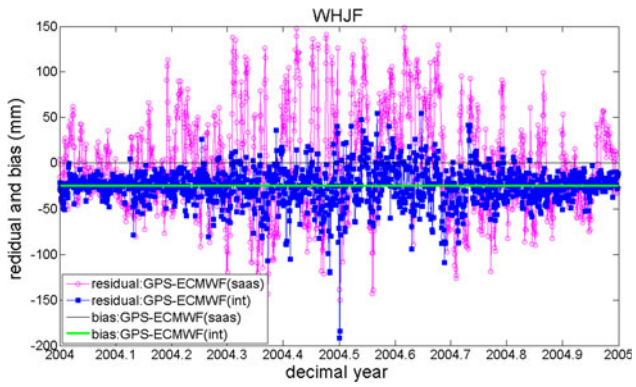


**Fig. 6** Comparison of bias and residuals for 2004 between GPS ZTD at the station WHJF and ECMWF ZTD with integration method (int) and Saastamoinen method (saas). The temporal resolution of the ZTD time series is 6 h

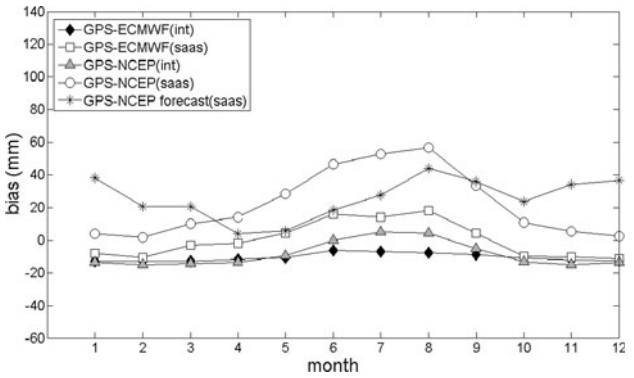


**Fig. 7** Monthly bias for 2004 between GPS ZTD and ECMWF/NCEP ZTD with integration method (int) and Saastamoinen method (saas)

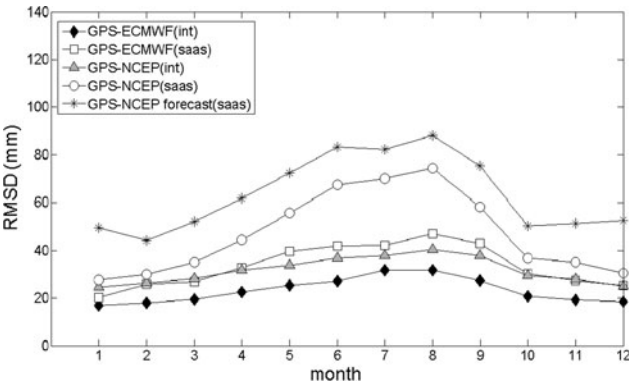


**Fig. 8** Monthly RMSD for 2004 between GPS ZTD and ECMWF/NCEP ZTD with integration method (int) and Saastamoinen method (saas)

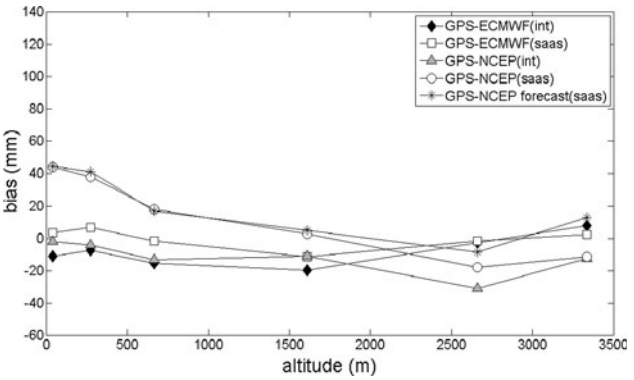


**Fig. 9** Variation of the yearly bias for 2004 between GPS ZTD and ECMWF/NCEP ZTD with integration method (int) and Saastamoinen method (saas) with the station altitude

between the bias and altitude difference between the station and nearest grid point is not obvious either (Fig. 10), which illuminates that the error in the retrieved ECMWF/NCEP ZTD is not caused by altitude difference. However, it is evident that the RMSD decreases with increasing GPS station altitude (Fig. 11). The reason is that the atmosphere becomes thinner at higher-altitude stations.

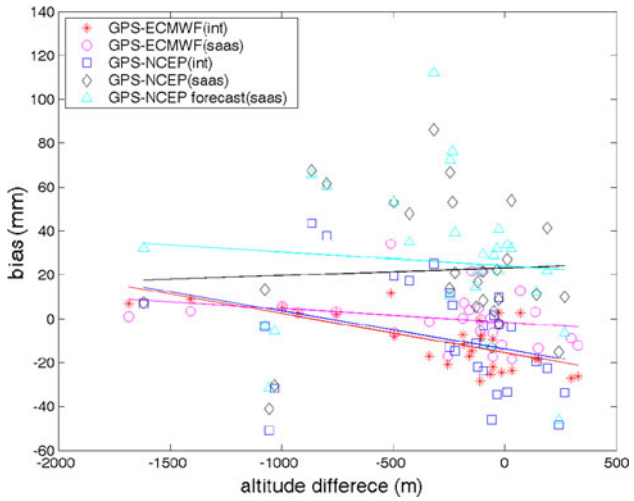


**Fig. 10** Variation of the yearly bias for 2004 between GPS ZTD and ECMWF/NCEP ZTD with integration method (int) and Saastamoinen method (saas) with the altitude difference (GPS—nearest grid point), and corresponding regression line

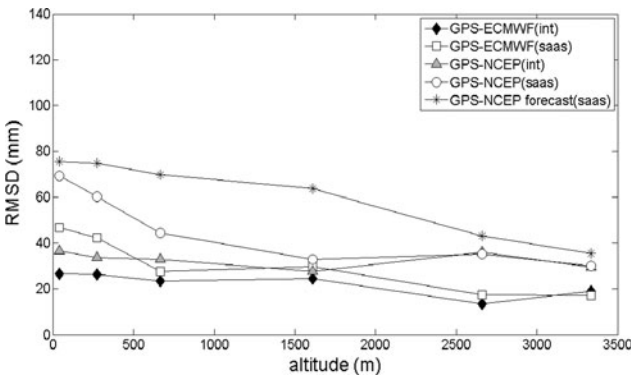


**Fig. 11** Variation of the yearly RMSD for 2004 between GPS ZTD and ECMWF/NCEP ZTD with integration method (int) and Saastamoinen method (saas) with the station altitude

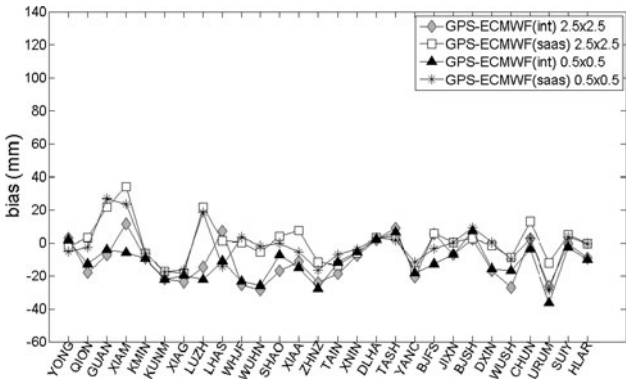


**Fig. 12** Yearly bias for 2004 between the GPS ZTD and ZTD derived from ECMWF data with resolutions 0.5° × 0.5° and 2.5° × 2.5° with integration method (int) and Saastamoinen method (saas)

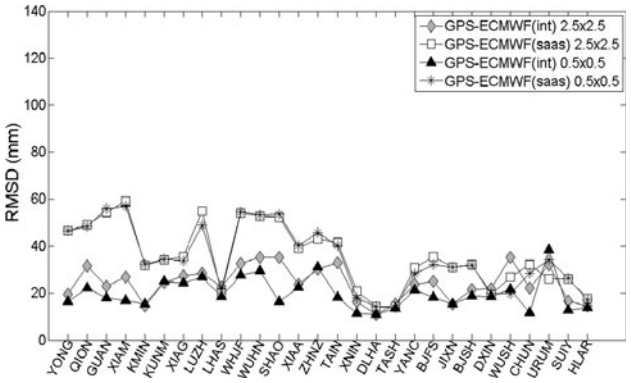


**Fig. 13** Yearly RMSD for 2004 between the GPS ZTD and ZTD derived from ECMWF data with resolutions 0.5° × 0.5° and 2.5° × 2.5° with integration method (int) and Saastamoinen method (saas)

**Table 3** Yearly bias and RMSD between GPS ZTD and ZTD derived from ECMWF data with different resolutions

| | dis (km) | alt dif (m) | bias (mm) | | RMSD (mm) | |
|---|---|---|---|---|---|---|
| | | | int | saas | int | saas |
| GPS-ECMWF 2.5 × 2.5 | | | | | | |
| Mean | 67 | −275 | −10.5 | 0.1 | 24.3 | 35.6 |
| Minimum | 6 | −1,684 | −0.6 | 0.1 | 10.8 | 14.2 |
| Maximum | 131 | 326 | −28.6 | 34.0 | 35.4 | 59.2 |
| GPS-ECMWF 0.5 × 0.5 | | | | | | |
| Mean | 16 | −230 | −11.9 | −2.1 | 19.8 | 35.1 |
| Minimum | 2 | −1,195 | 1.7 | 0.1 | 10.8 | 13.7 |
| Maximum | 26 | 144 | −36.7 | −28.7 | 38.4 | 57.2 |

The minimum and maximum values are given for the absolute values of the bias and the RMSD

In order to study the effect of the resolution of the meteorological data on the accuracy of ZTD acquired from the meteorological data, the bias and RMSD between GPS ZTD and ZTD from the ECMWF meteorological data with the horizontal resolution of 0.5° × 0.5° and 2.5° × 2.5° are compared and shown in Table 3. The yearly bias and RMSD with both resolutions at each GPS station are shown in Figs. 12 and 13.

Table 3 shows that the mean distance between the GPS station and the nearest grid point for the horizontal resolution of 0.5° × 0.5° is 16.3 km, whereas it is 67 km for the 2.5° × 2.5° resolution. The mean RMSD decreases by less than 4.5 mm, and the absolute value of the mean bias increases by only 1.4 mm. Similarly, we do not see large variations in the yearly bias or RMSD for the two resolutions at each GPS station from the figures.

## Conclusions

The ZTD derived from ECMWF/NCEP data has been validated by GPS ZTD in China. The following conclusions can be drawn:

1. When applying the integration method and Saastamoinen model method to derive ZTD from ECMWF/NCEP data, the former method yielded 1–3 cm better accuracy. Therefore, the integration method is recommended to derive ECMWF/NCEP ZTD for high-precision application.
2. The ZTD calculated from ECMWF by the integration method at GPS stations were compared with GPS ZTD. The bias ranged from 11.5 to −28.6 mm with a corresponding average of −10.5 mm, while the largest RMSD is 35.4 mm with an average of 24.3 mm. The bias between GPS ZTD and the ZTD calculated from NCEP by integration method ranges from 43.5 to −50.9 mm with an average of −8.5 mm, while the largest RMSD is 53.6 mm with a corresponding average of 33.0 mm. The agreement between GPS ZTDs and ECMWF ZTDs is better than that between GPS ZTDs and NCEP ZTDs. The ZTD derived from the ECMWF analysis or NCEP reanalysis pressure-level meteorological data can be used as the high-precision background field for a Chinese four-dimensional digital ZTD model.
3. The ZTD derived from NCEP surface forecast data has been compared with GPS ZTD. For most of the GPS stations, the bias and RMSD are less than 10 cm. It is suggested that the ZTD derived from NCEP prediction surface data can be used in most of GNSS navigation and positioning as real-time tropospheric delay correction.
4. The temporal and spatial distribution characteristics of the bias and RMSD between ECMWF/NCEP ZTD and GPS ZTD have been analyzed. The results show that the bias and RMSD, especially the RMSD, have seasonal variations. The RMSD values are generally higher in summer than winter. Furthermore, RMSD decreases as the altitude increases while its variation with latitude is not very obvious over the area of China.
5. After increasing the horizontal resolution of the ECMWF meteorological data from 2.5° × 2.5° to 0.5° × 0.5°, the RMSD in ZTD decreases by only about 1–5 mm and the bias has only 1 mm variation. This seems to demonstrate that the spatial structure of water vapor in China is slightly smaller than 2.5°.

**Acknowledgments** Data were provided by ECMWF and NCEP/NOAA/OAR/ESRL/PSD. PSD is the abbreviation of Physical Sciences Division from Earth System Research Laboratory (ESRL). The support from Keith Fielding (ECMWF) and Don Hooper (ESRL/PSD) is very much appreciated. Thanks to two anonymous reviewers and CIE for the constructive comments. This study was supported by funding from National Nature Science Foundation of China (No. 10603011), National High Technology Research and Development Program 863 (863 Program) (No. 2009AA12Z307), Science and Technology Commission of Shanghai Municipality (No. 05QMX1462, No.08ZR1422400), the Youth Foundation of Knowledge Innovation Project of the Chinese Academy of Sciences, Shanghai Astronomical Observatory (No. 5120090304), and Open Research Fund of State Key Laboratory of Information Engineering in Surveying, Mapping and Remote Sensing (No. 10P02).

## References

Andrei C, Chen R (2008) Assessment of time-series of troposphere zenith delays derived from the global data assimilation system numerical weather model. GPS Solut 13(2):109–117

Bromwich DH, Wang SH (2005) Evaluation of the NCEP–NCAR and ECMWF 15- and 40-year reanalyzes using rawinsonde data from two independent Arctic field experiments. Mon Weather Rev 133:3562–3578

Chao YC (1997) Real time implementation of the wide area augmentation system for the global positioning system with an emphasis on Ionospheric modeling. Ph.D. dissertation, Stanford University, Stanford

Ghoddousi-Fard R, Dare P, Langley RB (2009) Tropospheric delay gradients from numerical weather prediction models: effects on GPS estimated parameters. GPS Solut 13(4):281–291

Guerova G, Brockmann E, Quiby J, Schubiger F, Matzler C (2003) Validation of NWP mesoscale models with Swiss GPS network ANGENS. J Appl Meteorol 42(1):141–150

Haase JS, Vedel H, Ge M, Calais E (2001) GPS zenith troposphteric delay (ZTD) variability in the Mediterranean. Phys Chem Earth (A) 26(6–8):439–443

Herring TA, King RW, McClusky SC (2006) Document for the GAMIT GPS analysis software, release 10.3

Ibrahim HE, El-Rabbany A (2008) Regional stochastic models for NOAA-based residual tropospheric delays. J Navig 61:209–219

Kalnay E et al (1996) The NCEP/NCAR 40-year reanalysis project. Bull Am Meteor Soc 77:437–470
Liou Y-A, Huang CY (2000) GPS observation of PW during the passage of a typhoon. Earth Planets Space 52(10):709–712
Liou YA, Huang CY, Teng YT (2000) Precipitable water observed by ground-based GPS receivers and microwave radiometry. Earth Planets Space 52(6):445–450
Liou YA, Teng YT, Van Hove T, Liljegren J (2001) Comparison of precipitable water observations in the near tropics by GPS, microwave radiometer, and radiosondes. J Appl Meteor 40(1):5–15
Pany T, Pesec P, Stangl G (2001) Elimination of tropospheric path delays in GPS observations with the ECMWF numerical weather model. Phys Chem Earth Part A Solid Earth Geodesy 26(6–8):487–492
Pernigotti D, Rossa AM, Ferrario ME, Sansone M (2007) Application of a network of MW-radiometers and SODAR for the verification of meteorological forecasting models. Proceedings of the 6th UAQ international conference on urban air quality. Limassol, Cyprus
Saastamioinen J (1972) Contributions to the theory atmospheric refraction, Part II Refraction corrections in satellite Geodesy. Bull Geo 105:279–298
Shuli S, Wenyao Z, Jincai D, Xinhao L, Zhongyi C, Qixin Y (2004) Near Real-time sensing of PWV from SGCAN and the application test in numerical weather forecast. Chin J Geophys 40(4):719–727
Shuli S, Wenyao Z, Jincai D, Junhuan P (2005) 3D water vapor tomography with Shanghai GPS network to improve forecasted moisture field. Chin Sci Bull 50(20):2271–2277
Vedel H, Mogensen KS, Huang XY (2001) Calculation of zenith delays from meteorological data comparison of NWP model, radiosonde and GPS delays. Phys Chem Earth (A) 26(6–8): 497–502
Walpersdorf A, Bouin MN, Bock O, Doerflinger E (2007) Assessment of GPS data for meteorological application over Africa: study of error sources and analysis of positioning accuracy. J Atmos Solar-Terr Phys 69(12):1312–1330
Wang Q, Zhang P (2001) The initial result of crust movement observation network of China: GPS-derived velocity field (1998–2001), AGU Fall Meeting 2001

## Author Biographies

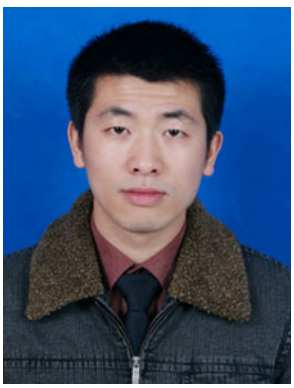

**Qinming Chen** is currently a PhD student. He graduated from Northeastern University, P.R.C., in 2002, and then worked as an assistant and project manager at the Southwest University of Science and Technology, P.R.C., from 2002 to 2007. He is now a PhD student (mainly focusing on geodesy and atmospheric remote sensing with ground-based GPS, etc.) at the ShanghaiAstronomical Observatory, Chinese Academy of Sciences.

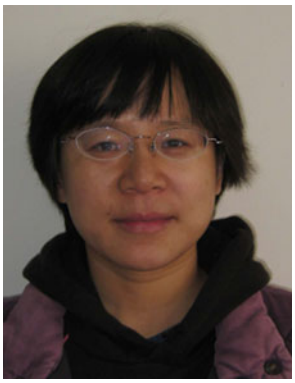

**Shuli Song** is currently an associate research fellow. She has obtained her PhD degree in 2004 from the Shanghai Astronomical Observatory, Chinese Academy of sciences. Her main research interests are in geodesy and atmospheric/ionospheric remote sensing with ground-based GPS.

**Stefan Heise** (*30.05.1973) studied meteorology at the Free University of Berlin from 1994 to 1998 (graduation diploma). From 1998 to 2002, he was a PhD student (ionospheric remote sensing with space-borne GPS observations aboard CHAMP) and project scientist at the German Aerospace Center (DLR), Institute of Communications and Navigation in Neustrelitz. After conferral of a doctorate (Dr. rer. Nat., Free University of Berlin) in 2002, he has worked at the GFZ German Research Centre for Geosciences (Potsdam). His scientific work is focused on atmospheric/ionospheric remote sensing with space- and ground-based GPS.

**Yuei-An Liou** (S'91, M'96, SM'01) received his BS degree in electrical engineering from the National Sun Yat-Sen University, Kaohsiung, Taiwan, MSE degree in electrical engineering (EE), MS degree in atmospheric and space sciences and PhD degree in EE and atmospheric, oceanic and space sciences from the University of Michigan, Ann Arbor, in 1987, 1992, 1994 and 1996, respectively. He is now a professor of the Center for Space and Remote Sensing Research (CSRSR), National Central University, Taiwan. He was awarded Honorary Life Member of The Korean Society of Remote Sensing in 2007. He was elected Foreign Member, Russian Academy of Engineering Sciences in 2008. He was awarded Outstanding Alumni Awards by University of Michigan Alumni Association in Taiwan and National Sun Yat-sen University in 2008. He was elected Academician, International Academy of Astronautics in 2009. He was honored as Distinguished Professor, National Central University in 2010.

**Wenyao Zhu** is a senior research scientist and professor at the Shanghai Astronomical Observatory, Chinese Academy of sciences. His research mainly focuses on satellite dynamics, satellite geodesy and geodynamics.

**Jingyang Zhao** graduated from the China University of Geosciences Beijing in 2009. She is now a student at the Shanghai Astronomical Observatory, Chinese Academy of Sciences, studying for her master's degree in atmospheric remote sensing with ground-based GPS.